

MIT Open Access Articles

A two-dimensional model of low-Reynolds number swimming beneath a free surface

The MIT Faculty has made this article openly available. **Please share** how this access benefits you. Your story matters.

Citation: Crowdy, Darren et al. "A Two-dimensional Model of low-Reynolds Number Swimming Beneath a Free Surface." *Journal of Fluid Mechanics* 681 (2011): 24–47.

As Published: <http://dx.doi.org/10.1017/jfm.2011.223>

Publisher: Cambridge University Press

Persistent URL: <http://hdl.handle.net/1721.1/78605>

Version: Author's final manuscript: final author's manuscript post peer review, without publisher's formatting or copy editing

Terms of use: Creative Commons Attribution-Noncommercial-Share Alike 3.0



A two-dimensional model of low-Reynolds number swimming beneath a free surface

Darren Crowdy,¹ Sungyon Lee,² Ophir Samson,¹ Eric Lauga,³ and A. E. Hosoi²

¹*Department of Mathematics, Imperial College, London, SW7 2AZ, United Kingdom*

²*Hatsopoulos Microfluids Laboratory, Department of Mechanical Engineering,
Massachusetts Institute of Technology, 77 Massachusetts Avenue, Cambridge, MA 02139, USA*

³*Department of Mechanical and Aerospace Engineering,
University of California San Diego, 9500 Gilman Drive, La Jolla CA 92093-0411, USA.*

(Dated: March 24, 2010)

Biological organisms swimming at low Reynolds number are often influenced by the presence of rigid boundaries and soft interfaces. In this paper we present an analysis of locomotion near a free surface with surface tension. Using a simplified two-dimensional singularity model, and combining a complex variable approach with conformal mapping techniques, we demonstrate that the deformation of a free surface can be harnessed to produce steady locomotion parallel to the interface. The crucial physical ingredient lies in the nonlinear hydrodynamic coupling between the disturbance flow created by the swimmer and the free boundary problem at the fluid surface.

I. INTRODUCTION

Low-Reynolds number swimming near solid boundaries or interfaces can exhibit interesting and unexpected features. In particular, the presence of long-range interactions typical of flows at low Reynolds numbers implies that, in general, boundary effects can not be ignored [1, 2]. For instance, *E. coli* cells are observed to change their swimming trajectories from straight to circular when they are moving parallel to a solid surface [3–6], a behaviour modification which may have important implications in the formation of biofilms [7]. The motion of microorganisms near soft interfaces, such as spermatozoa motility through the mucus-filled female reproductive track [8], is even more intriguing as the nonlinear coupling between the motion of the swimmer and the changing shape of the interfaces adds an extra level of complexity to the problem.

The study of low Reynolds number swimmers near a no-slip wall has received considerable attention in the past, and we refer to the reviews by [1] and [2] for a discussion of the relevant literature. Most theoretical work has focused on quantifying the change in swimming speed and energetics near solid boundaries [9–13]. More recent work has addressed the dynamics of confined swimmers, and tackled the subtle interplay between the time evolution of a swimmer’s orientation and its position. For example, a well-known feature of swimming near a solid boundary is that organisms moving at low Reynolds number tend to be attracted to solid surfaces [13–19]. This phenomenon can be rationalized by a fundamentally hydrodynamical mechanism in which the interaction with the rigid boundary causes a swimmer to reorient itself in such a way that it is eventually attracted to its hydrodynamic image system in the wall [19].

Other studies have revealed additional dynamical features of a swimmer’s behaviour near a wall. [20] have conducted numerical experiments to understand the wall-bounded dynamics of model swimmers from a control and dynamical systems perspective. In addition to the existence of a steady state in which the swimmers travel in a steady rectilinear motion parallel to the wall, the authors found that the generic motion of a swimmer can be described by nonlinear periodic orbits along the wall with complicated spatio-temporal structure. These observations have since been corroborated by laboratory experiments involving small robotic swimmers in a tank of viscous fluid [21]. Motivated by these studies, [22] have recently proposed a simple two dimensional model of a swimmer near a wall. Using a complex variable formulation of the problem, they obtained results in agreement with those of [20] and [21].

In the current paper, we address the coupling between a low-Reynolds swimmer and a surface which can deform, and focus on the case of a free interface with surface tension. Previous work considered how the *unsteady* deformation of soft surfaces generated by time-reversible flows could provide new modes of locomotion and pumping [23]. Here we ask the following question: Can a low-Reynolds number body exploit the deformation of a free surface to swim steadily? To emphasize the role played by the surface deformation, we consider swimmers which cannot swim in the absence of a free surface, and determine whether they are able, through the disturbance flow field they are creating and the subsequent surface deformation, to acquire locomotive abilities. Specifically, using the modeling approach of

[22], we focus on identifying a steady mode of locomotion in which a swimmer translates at a constant speed parallel to the undisturbed free surface. Since, in the neighborhood of a flat no-slip wall, the motion of a swimmer generically follows a time-dependent periodic orbit, it is not clear a priori that a steadily translating swimmer motion beneath a free capillary surface is possible. What we show below is that such a mode of locomotion is indeed possible and, within our model can be described in a mathematically explicit way.

Our study was originally motivated by the discovery of a peculiar mode of locomotion employed by water snails that crawl underneath the free surface. Separated from the interface by a thin layer of mucus, these organisms deform their foot to create a lubrication flow inside the mucus layer. This flow results in deformations of the free surface, which in turn rectifies the flow, allowing the water snails to move [24]. The analysis in this paper contained two significant constraints, namely the gap between the swimmer and the air-water interface was assumed to be thin, and the deformation of the free surface was assumed to asymptotically small. The work in the current paper removes these constraints and considers a more general mechanism for a swimmer translating steadily beneath the free surface.

Low Reynolds number swimmers exert no net force and no net torque on the flow, and it is precisely these constraints that dictate the subsequent speed of the swimmer and its angular velocity. Here we introduce a mathematical representation of the swimmer as a two-dimensional torque-free point stresslet which, by definition, is force and torque-free. This type of singularity model has been widely used in modeling suspensions of force-free particles [25] and swimming microorganisms [18, 26, 27]. The approach is equivalent to considering the swimmer on distances much larger than its intrinsic size, so that its precise geometric structure and the fine details of its swimming protocol are encapsulated in the effective far-field multipole structure. The two-dimensional assumption, although idealized and not directly relevant to biological swimmers, allows us to explicitly solve for the nonlinear free boundary problem, thereby shedding light on this new mode of locomotion.

Our mathematical approach is inspired by the work of [28] who considered surface deformations generated by two counter-rotating cylinders beneath a free surface at low Reynolds numbers. In a similarly idealized model, the flow generated by the two counter-rotating cylinders is modeled by a single potential dipole located on the axis of symmetry of the deformed free surface. This flow results in symmetric deformations of the interface which are calculated, for a given dipole strength and fluid properties, by means of conformal mapping methods. Notably, the conformal map approach allowed them to produce exact solutions even for large nonlinear deformations of the free surface. Furthermore, their analytic results exhibit remarkable agreement with the experimental data of free surface deformations for different rotation rates of the cylinders. In the spirit of [28] we therefore use a conformal map to solve for the shapes of the free surface governed by the interaction between surface tension and the flow field generated by the swimmer, represented as a combination of singularities. The difference here is that we must allow for non symmetric deformations of the interface and adapt the analysis to admit a stresslet singularity in the fluid (rather than a potential dipole).

This paper is organized as follows. In §II, the two dimensional Stokes equations and relevant boundary conditions are introduced in complex variables. The singularity model approach is then explained in §III. Section IV uses a method of images to demonstrate that steady motion of a swimmer beneath a flat undeformed interface is not possible. Section V then introduces a conformal mapping approach that enables us to explore solutions in which the free surface admits essentially arbitrary deformations. Section VI gives a characterization of the class of steadily translating solutions, and is followed by the conclusions in §VII.

II. COMPLEX VARIABLE FORMULATION OF STOKES FLOW

Let the two-dimensional quiescent fluid occupy the area beneath a deformable fluid-air interface, D . The fluid is assumed to be incompressible and, in the Stokes régime, the streamfunction $\hat{\psi}$ is known to satisfy the biharmonic equation

$$\nabla^4 \hat{\psi}(\hat{x}, \hat{y}) = 0. \quad (1)$$

Introducing the complex-valued coordinate $\hat{z} = \hat{x} + i\hat{y}$, it is possible to write the general solution of the biharmonic

equation in the form

$$\hat{\psi} = \text{Im}[\bar{\hat{z}}\hat{f}(\hat{z}) + \hat{g}(\hat{z})]. \quad (2)$$

Here $\hat{f} \equiv \hat{f}(\hat{z})$ and $\hat{g} \equiv \hat{g}(\hat{z})$ are two functions which must be analytic functions of \hat{z} inside the fluid region except at isolated points where singularities are deliberately introduced in order to model particular flow conditions. These functions are sometimes referred to as *Goursat functions*.

It is possible [29] to express all the usual physical variables in terms of these two functions. Indeed, it can be shown that

$$\begin{aligned} \frac{\hat{p}}{\mu} - i\hat{\omega} &= 4\hat{f}'(\hat{z}), \\ \hat{u} + i\hat{v} &= -\hat{f}(\hat{z}) + \overline{\hat{z}\hat{f}'(\hat{z})} + \overline{\hat{g}'(\hat{z})}, \\ \hat{e}_{11} + i\hat{e}_{12} &= \overline{\hat{z}\hat{f}''(\hat{z})} + \overline{\hat{g}''(\hat{z})}. \end{aligned} \quad (3)$$

Here, \hat{p} is the fluid pressure, $\hat{\omega}$ is the vorticity, (\hat{u}, \hat{v}) is the fluid velocity and \hat{e}_{ij} is the fluid rate-of-strain tensor. The dynamic fluid viscosity is μ . Primes denote differentiation with respect to \hat{z} , and overbars denote complex conjugates.

The stress boundary condition on the free surface requires that the normal fluid stress is balanced by the surface tension and that the tangential stress vanishes. This can be written as

$$-\hat{p}n_i + 2\mu\hat{e}_{ij}n_j = \sigma\kappa n_i \quad (4)$$

where σ is the surface tension, κ is the surface curvature, and n_i is the outward unit vector normal to the interface. In addition, the kinematic condition on the interface requires that the normal velocity of the interface equals the normal fluid velocity.

The governing equations, Goursat functions, and corresponding boundary conditions are non-dimensionalized as follows:

$$\begin{aligned} \hat{z} &= \hat{h}z, & \hat{z}_d &= \hat{h}z_d, & \hat{u} + i\hat{v} &= \hat{U}(u + iv), & \hat{\psi} &= \hat{U}\hat{h}\psi, \\ \hat{f} &= \hat{U}f, & \hat{g} &= \hat{U}\hat{h}g, & \hat{p} &= \frac{\mu\hat{U}}{\hat{h}}p, \end{aligned} \quad (5)$$

where \hat{z}_d is the dimensional location of the swimmer, \hat{h} is the magnitude of \hat{z}_d or the vertical distance of the swimmer from the interface, and \hat{U} is a characteristic speed of translation. The capillary number Ca , which reflects the dimensionless ratio of viscous to capillary effects, is defined as

$$\text{Ca} = \frac{\mu\hat{U}}{\sigma}. \quad (6)$$

It can be shown that the complex form of the stress condition (4) on the air-fluid interface is equivalent to the relation

$$\frac{dH}{ds} = -\frac{i}{2\text{Ca}} \frac{d^2z}{ds^2}, \quad (7)$$

where ds is a differential element of arc length along the free surface and

$$H \equiv f(z) + z\bar{f}'(\bar{z}) + \bar{g}'(\bar{z}). \quad (8)$$

Hence, the stress condition can be integrated once with respect to s to give

$$f(z) + z\bar{f}'(\bar{z}) + \bar{g}'(\bar{z}) = -\frac{i}{2\text{Ca}} \frac{dz}{ds}, \quad (9)$$

where, without loss of generality, the constant of integration has been set equal to zero.

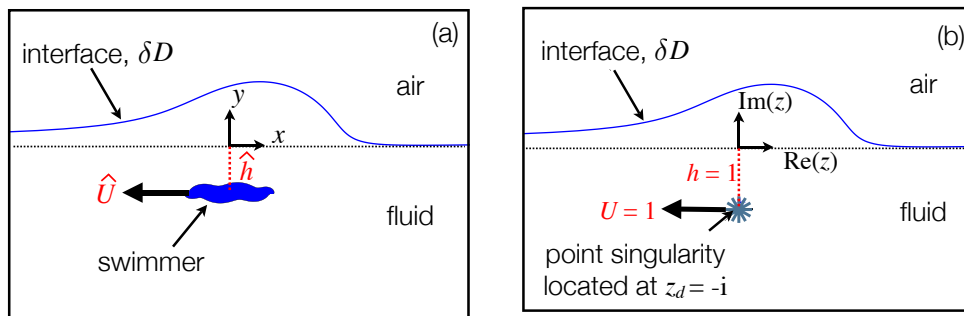


FIG. 1: Illustration of the singularity model: A finite-body swimmer beneath a free surface is modelled as a point stresslet singularity with superposed potential dipole and quadrupole.

III. A SINGULARITY MODEL OF THE SWIMMER

From the first equation in (3) it is clear that singularities of the Goursat function $f(z)$ will be related to local singularities in the pressure field and hence, to localized force singularities. A *logarithmic* singularity of $f(z)$ corresponds to what is often referred to as a *stokeslet*, or point force singularity [30] which, as previously discussed, is not allowed owing to the condition that the swimmer exerts no net force on the flow.

The next order singularity (the derivative of the logarithm) is a simple pole. If near z_d , $f(z)$ has a simple pole singularity,

$$f(z) = \frac{s^*}{z - z_d} + \text{analytic}, \quad (10)$$

then, in order to ensure that the velocity field scales like $1/|z - z_d|$ (rather than $1/|z - z_d|^2$) we must also have

$$g'(z) = \frac{s^* \bar{z}_d}{(z - z_d)^2} + \text{analytic}. \quad (11)$$

Thus, if $f(z)$ and $g'(z)$ locally have the behavior (10) and (11) respectively near z_d then there is a *stresslet* of strength s^* at z_d . In general, if $g(z)$ has a simple pole near some point z_d of the form

$$g(z) = \frac{d}{z - z_d} + \text{analytic}, \quad (12)$$

then we say there is a *dipole* of strength d at z_d . A stresslet singularity of strength s^* at z_d therefore corresponds to a simple pole of $f(z)$ at z_d with residue s^* together with a simple pole of $g(z)$ with residue $-s^* \bar{z}_d$ at the same point.

There is a physical way to understand this singularity of $f(z)$. Swimmers at low Reynolds numbers propel themselves by exerting a local force on the flow (for example, the waving flagellum of a spermatozoa) which is then counterbalanced by a net drag on its body (the head of the spermatozoa plus its flagellum) leaving the total net force on it equal to zero [e.g. see review in 2]. If this scenario is modeled as two logarithmic singularities of $f(z)$ (two point forces) drawing infinitesimally close together with equal and opposite strengths tending to infinity at a rate inversely proportional to their separation, the limit is precisely a simple pole singularity of $f(z)$ of the form (10).

In a general singularity description of a swimmer, $g'(z)$ is also singular at z_d . We already know it must have a second order pole (11) (this is associated with the stresslet) but it can have additional singularities. The singularities of $g(z)$ are *potential* multipoles because, as is clear from (3), only the singularities of $f(z)$ contribute to the vorticity of the flow. Different swimmers generate different effective singularities according to their particular swimming protocol. Any choice of singularities that we assume $g'(z)$ to have at z_d is therefore a manifestation of our choice of swimmer type. It is not clear, *a priori*, how to pick either the type of these singularities of $g'(z)$ or their magnitudes.

In this paper we adopt the same singularity model of a swimmer used by [22] in their studies of a low-Reynolds number swimmer near a no-slip wall. They motivated their choice of singularities by considering a concrete model of

a finite-area circular “treadmilling” swimmer of radius ϵ . It was supposed that, on its surface, the swimmer generates a purely tangential surface velocity given by

$$U(\phi, t) = 2V \sin(2(\phi - \theta(t))) \quad (13)$$

where V is a constant (setting the time-scale of the swimmer’s motion), ϕ is the angular variable and $\theta(t)$ is a distinguished angle taken to be the direction in which the head of the swimmer is pointed. By solving a boundary value problem for the flow associated with this swimmer in an unbounded Stokes flow, it is possible to show that such a swimmer has an effective singularity description consisting of a stresslet of strength $\mu(t) = \epsilon V \exp(2i\theta(t))$ with a superposed potential quadrupole of strength $2\mu(t)\epsilon^2$.

This model is a particular case of a general class of simplified swimmers first considered in a theoretical study due to [31] who looked at the effect of imposing velocity profiles of general form on the surface of a circular swimmer. Such an “envelope model” captures the macroscopic effect of the motion of many small-scale beating cilia on the swimmer surface. Similarly, cilia-aided crawling of organisms beneath a free surface has been observed in nature, in particular for some families of snails. [32] concluded that the locomotion of *Alectrion trivittata*, which crawls upside down on the surface, relies solely on the ciliary action. He conducted a similar study on *Polinices duplicata* and *Polinices heros*, both of which were observed to use both cilia and muscle contraction for locomotion on hard surfaces [33]. Only ciliary motion was employed by the young *Polinices heros* when crawling inverted beneath the surface.

Prompted by the success of the previously described singularity model, we extend the study to point swimmers (beneath a free surface) within the same general class: that is, a point stresslet superposed with a potential dipole and quadrupole. The dipole has been included because it is a lower order singularity than the quadrupole and there is no reason *a priori* to suppose it is absent (moreover steady rectilinear motion is expected to involve a dipole in its singularity description). This means that we will seek $f(z)$ and $g(z)$ with the functional forms

$$f(z) = \frac{s^*}{z+i} + f_0 + f_1(z+i) + \dots, \quad g(z) = \frac{q^*}{(z+i)^2} + \frac{(-is^* + d^*)}{(z+i)} + g_0 + g_1(z+i) + \dots \quad (14)$$

where the singularity is at $z = -i$ and f_0, f_1, g_0 and g_1 are constants. We will refer to s^* as the stresslet strength, q^* as the quadrupole strength and d^* as the dipole strength (note that part of the coefficient of $1/(z+i)$ in $g(z)$ is naturally associated with the stresslet singularity as seen in (10) and (11)). We will not make any *a priori* assumptions on the relative magnitudes of s^*, d^* and q^* since, for a steady solution, we expect these to be determined by the conditions for equilibrium.

[22] show that the evolution equations for the swimmer position $z_d(t)$ and its orientation $\theta(t)$ are given by the dynamical system

$$\frac{dz_d(t)}{dt} = -f_0 + z_d \overline{f_1} + \overline{g_1}, \quad \frac{d\theta(t)}{dt} = -2\text{Im}[f_1]. \quad (15)$$

The first equation states that the swimmer moves with the finite part of the fluid velocity at the swimmer position, while the second equation states that its angular velocity equals half the regular part of the vorticity at the swimmer position. In the present paper we adopt these same evolution equations but focus on finding equilibrium solutions in which the swimmer translates steadily in the direction of the undeformed interface (i.e., parallel to the x -axis). In a co-travelling frame we therefore need to find solutions satisfying the conditions

$$0 = -f_0 + z_d \overline{f_1} + \overline{g_1}, \quad 0 = \text{Im}[f_1]. \quad (16)$$

The first equation ensures that the swimmer is stationary in the co-moving frame. The second equation ensures that the local vorticity at the swimmer position vanishes so that its orientation remains fixed in time. Note that for a no-slip wall the time evolution of the swimmer’s orientation proves to be a crucial ingredient in understanding the dynamics of swimmers near those surfaces [19], and the same is expected to be true near a free surface.

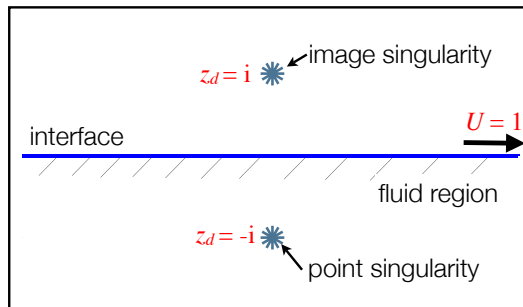


FIG. 2: The method of images near a flat free surface: to satisfy the boundary condition on the surface an image singularity must be introduced at the reflection of the point swimmer position.

IV. STEADY SWIMMING BENEATH A FLAT INTERFACE: METHOD OF IMAGES

It is instructive to first examine whether it is possible to find a solution for a point swimmer (of the type just described) translating steadily beneath a flat undeformed interface. To do so we must seek $f(z)$ and $g(z)$ satisfying the boundary conditions on the free surface, with singularities of the form (14), and satisfying conditions (16). Owing to the simplicity of the geometry we search for such a solution using the method of images, as originally introduced by Blake and co-workers for three-dimensional flows near no-slip walls [34, 35]. We now demonstrate that such a solution does not exist. In subsequent sections we succeed in identifying steadily translating solutions in which the interface deforms. This highlights the crucial role played by the deformability of the interface in providing a mechanism for steady translation of the swimmer.

Consider a swimmer moving at a prescribed horizontal speed $U = -1$ beneath a flat interface in a Stokes flow with no background flow. It is convenient to work in a frame traveling with the swimmer. Then the swimmer is stationary at $z_d = -i$ while the fluid in the far-field has unit speed in the x -direction.

We seek a solution of the form

$$f(z) = \frac{s^*}{z+i} + \frac{\hat{s}^*}{z-i} + f_0 \quad (17)$$

where, in addition to the stresslet of strength s^* at $z_i = -i$, we have placed an image stresslet of strength \hat{s}^* (to be determined) at $z = i$ and f_0 is a constant. Figure 2 shows a schematic of both the swimmer and its image. The form of $g'(z)$ is now forced by the stress boundary condition on this interface. On $\bar{z} = z$ we have, from (9),

$$\bar{g}'(z) = -f(z) - z\bar{f}'(z) + \frac{i}{2Ca}. \quad (18)$$

Substitution of (17) into (18) and picking $\hat{s}^* = \bar{s}^*$ so that $g'(z)$ has no rotlet contribution (no simple poles) leads to

$$g'(z) = -\frac{is^*}{(z+i)^2} + \frac{i\bar{s}^*}{(z-i)^2} + g_0 \quad (19)$$

which we rewrite as

$$g'(z) = \left[\frac{is^*}{(z+i)^2} - \frac{i\bar{s}^*}{(z-i)^2} \right] - \frac{2is^*}{(z+i)^2} + \frac{2i\bar{s}^*}{(z-i)^2} + g_0. \quad (20)$$

As can be seen by comparison of (17) and (20) with (10) and (11), the two second order poles in square brackets are associated with the two stresslets (the swimmer stresslet and its image) and the additional second order poles correspond to superposed potential dipole singularities (one at the swimmer position and another at the image point).

The constants f_0 and g_0 must be picked so that the far-field velocity condition is satisfied. Making use of (17) and (18) in the expression for the velocity (3) in the far field equation produces

$$-f_0 + \bar{g}_0 = 1. \quad (21)$$

By balancing the constant terms in the stress condition, we can deduce

$$f_0 = -\frac{1}{2} + \frac{i}{4\text{Ca}}, \quad g_0 = \frac{1}{2} - \frac{i}{4\text{Ca}}. \quad (22)$$

Finally, the swimmer must be stationary in the cotranslating frame. Hence the finite part of

$$-f(z) + z\overline{f}'(\overline{z}) + \overline{g}'(\overline{z}) \quad (23)$$

at $z = -i$ must vanish. This leads to

$$0 = -\frac{\overline{s^*}}{(-2i)} - f_0 + \frac{is^*}{(-4)} - \frac{is^*}{(-4)} + \overline{g_0} \quad (24)$$

and the conclusion that

$$s^* = 2i. \quad (25)$$

Note that the strength of these singularities does not depend on the capillary number.

The solutions for $f(z)$ and $g'(z)$ just derived give the instantaneous velocity field. We must also check that the free surface is a streamline. It can be verified (see the discussion in the next section) that this condition is equivalent to

$$g(z) + \overline{z}f(z) = 0 \quad (26)$$

on the real axis. By making use of (17) and (18) we find

$$\begin{aligned} g(z) + z\overline{f}(z) &= \frac{is^*}{(z+i)} - \frac{i\overline{s^*}}{(z-i)} + zg_0 + \frac{zs^*}{(z+i)} + \frac{z\overline{s^*}}{(z-i)} + zf_0 \\ &= 2\text{Re}[s^*] = 0 \end{aligned}$$

which confirms that the free surface is indeed a streamline.

It still remains to satisfy the condition that $\text{Im}[f_1] = 0$ but it is easily verified that this condition is not satisfied. Furthermore, there are no further degrees of freedom in the solution that will allow us to enforce it. We therefore conclude that steady, non-rotating solutions for a steadily translating swimmer beneath an undeformed interface do not exist.

V. STEADY SWIMMING BENEATH A DEFORMED INTERFACE: CONFORMAL MAPPING

The failure to identify a solution for a steadily translating swimmer beneath an undeformed interface does not preclude the existence of such solutions when the interface deforms. We now seek such solutions. When the interface is not flat it is no longer obvious how to apply the method of images. Instead, we introduce a new solution method based on conformal mapping. This enables us to successfully resolve the nonlinear interaction between the point swimmer and the deformed free surface.

Consider the unit disc $|\zeta| \leq 1$ in a complex parametric ζ -plane. It is known, by the Riemann mapping theorem [36], that there exists a conformal mapping $z(\zeta)$ that will map this unit disc to the fluid region beneath the free surface. The free surface itself will be the image of the unit circle $|\zeta| = 1$ under this mapping (see Figure 3). Since the physical fluid domain is unbounded and the free surface extends to infinity, there must be a simple pole of $z(\zeta)$ on the unit ζ -circle. Using a rotational degree of freedom of the Riemann mapping theorem, we take this pole to be at $\zeta = -i$. The most general form of the mapping can then be represented as

$$z(\zeta) = \frac{a}{\zeta + i} + \sum_{k=0}^{\infty} a_k \zeta^k \quad (27)$$

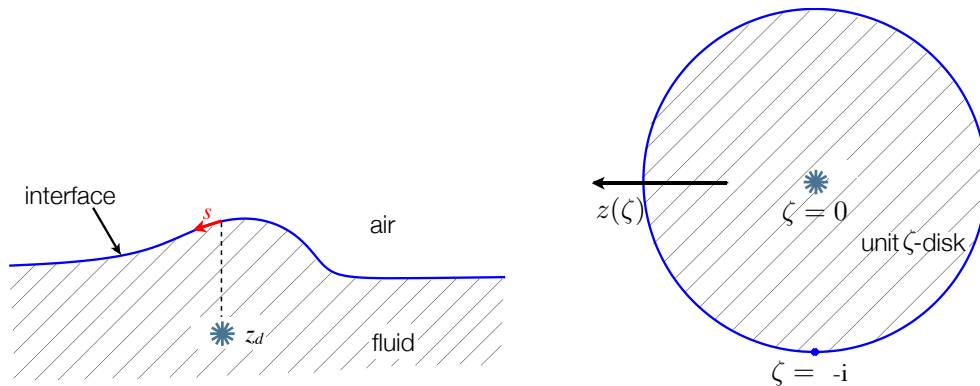


FIG. 3: Conformal mapping $z(\zeta)$ from the unit ζ -disk to the fluid region beneath the interface. In this mapping, $\zeta = 0$ maps to the swimmer at $z = z_d$, and $\zeta = -i$ maps to the interface at infinity. The variable s denotes the arclength and increases as shown in the figure.

where a and $\{a_k\}$ are a (generally infinite) set of complex coefficients. For a one-to-one function, it must also be true that $dz/d\zeta \neq 0$ inside the unit disc. There are two remaining degrees of freedom in the mapping theorem which allow us to prescribe that the singularity z_d corresponding to the swimmer is the image of $\zeta = 0$, i.e,

$$z_d = z(0). \quad (28)$$

This means that the pre-image of z_d is the point $\zeta = 0$.

We seek a solution where the singularity travels uniformly with speed $U = -1$ in the x -direction and we again move to a co-travelling frame in which both the swimmer and the shape of the free surface are stationary. The kinematic condition on the interface for a steady solution in this frame is

$$\mathbf{u} \cdot \mathbf{n} = 0. \quad (29)$$

If the normal vector $\mathbf{n} = (n_x, n_y)$, the complex normal $n_x + in_y$ is $-idz/ds$, where s increases along the interface from positive infinity to negative (see Figure 3). Using this fact, (29) can be expressed in the complex form as

$$\text{Re} \left[(u + iv)i \frac{d\bar{z}}{ds} \right] = 0. \quad (30)$$

This condition is equivalent to the free surface being a streamline and, in turn, corresponds to the following condition at the free surface:

$$\bar{z}f(z) + g(z) = 0. \quad (31)$$

The easiest way to show this is to compute the derivative (with respect to arclength s) of the quantity $\bar{z}f(z) + g(z)$ on the interface and then make use of (9) and (30) to show that $\bar{z}f(z) + g(z)$ equals zero.

In the far-field it is required that

$$f(z) \rightarrow f_\infty + \frac{f_\infty^{(1)}}{z} + \dots \quad \text{and} \quad g'(z) \rightarrow g_\infty + \frac{g_\infty^{(1)}}{z} + \dots \quad (32)$$

so that, as $z \rightarrow \infty$,

$$u + iv \rightarrow -f_\infty + \overline{g_\infty} + \mathcal{O}(|z|^{-1}). \quad (33)$$

To satisfy the boundary conditions at infinity that the interface moves in the x -direction with unit speed we must have

$$-f_\infty + \overline{g_\infty} = 1. \quad (34)$$

It can be shown that

$$f_\infty = -\frac{1}{2} + \frac{i}{4\text{Ca}} \quad \text{and} \quad g_\infty = \frac{1}{2} - \frac{i}{4\text{Ca}}. \quad (35)$$

To see how these relations arise, we make use of the fact that

$$\frac{dz}{ds} = \frac{i\zeta z_\zeta}{|z_\zeta|} \quad (36)$$

and show that, as $\zeta \rightarrow -i$,

$$-\frac{i}{2} \frac{dz}{ds} \rightarrow \frac{i}{2\text{Ca}} \frac{a}{|a|} \quad (37)$$

so that, using the condition (9), as $\zeta \rightarrow -i$,

$$f_\infty + \overline{g_\infty} = \frac{i}{2\text{Ca}} \frac{a}{|a|}. \quad (38)$$

Since, as $\zeta \rightarrow -i$ on $|\zeta| = 1$,

$$\overline{z} = \overline{z}(\zeta^{-1}) = \frac{\overline{a}\zeta}{1-i\zeta} + \overline{a_0} + \frac{\overline{a_1}}{\zeta} = \frac{\overline{a}}{\zeta+i} + i\overline{a} + \overline{a_0} + \frac{\overline{a_1}}{\zeta} \rightarrow \frac{\overline{a}z}{a} + \dots \quad (39)$$

it also follows, from (31), that

$$g(z) \rightarrow -\frac{f_\infty \overline{a}z}{a}, \quad (40)$$

and hence

$$g_\infty = -\frac{f_\infty \overline{a}}{a}. \quad (41)$$

This means, from (34), that

$$-f_\infty - \frac{\overline{f_\infty} a}{\overline{a}} = 1. \quad (42)$$

The only way for the velocity to be purely real is for a to be real so that

$$-f_\infty - \overline{f_\infty} = 1. \quad (43)$$

It further follows, from (38), that

$$f_\infty - \overline{f_\infty} = \frac{i}{2\text{Ca}}, \quad (44)$$

leading to (35).

Together with the stress condition (9), the kinematic condition (29) can be written as

$$\text{Re} \left[2f i \overline{\left(\frac{dz}{ds} \right)} \right] = \frac{1}{2\text{Ca}}. \quad (45)$$

We now introduce the composed functions

$$F(\zeta) \equiv f(z(\zeta)), \quad G(\zeta) \equiv g(z(\zeta)), \quad (46)$$

which can be used in the kinematic condition together with (36) to give

$$\text{Re} \left[\frac{2F(\zeta)}{\zeta z_\zeta} \right] = \frac{1}{2\text{Ca}|z_\zeta|}, \quad (47)$$

where $z_\zeta(\zeta) \equiv dz/d\zeta$. Since $f(z)$ is required to have a simple pole at z_d , $F(\zeta)$ must have a simple pole at $\zeta = 0$. Therefore

$$F(\zeta) = \frac{F_d}{\zeta} + F_0 + \mathcal{O}(\zeta) \quad (48)$$

for some constant F_d (to be determined). Therefore, consider

$$\operatorname{Re} \left[\frac{F(\zeta)}{\zeta z_\zeta} - \frac{D}{\zeta^2} - \frac{C}{\zeta} \right] = \frac{1}{4\operatorname{Ca}|z_\zeta|} - \operatorname{Re} \left[\frac{D}{\zeta^2} + \frac{C}{\zeta} \right] = \frac{1}{4\operatorname{Ca}|z_\zeta|} - \operatorname{Re} \left[\overline{D}\zeta^2 + \overline{C}\zeta \right]. \quad (49)$$

For suitable choices of constants C and D the function in the square brackets on the left hand side of (49) is analytic everywhere inside the unit ζ -disc. Equation (49) therefore gives the real part of an analytic function on the boundary of the disc. The Poisson integral formula can be used to give

$$F(\zeta) = \zeta z_\zeta(\zeta) \left[I(\zeta, \operatorname{Ca}) + \frac{D}{\zeta^2} + \frac{C}{\zeta} - \overline{D}\zeta^2 - \overline{C}\zeta + ib \right], \quad (50)$$

where b is some real constant and

$$I(\zeta, \operatorname{Ca}) = \frac{1}{8\pi i \operatorname{Ca}} \oint_{|\zeta'|=1} \frac{d\zeta' \zeta' + \zeta}{\zeta' \zeta' - \zeta} \frac{1}{|z_\zeta(\zeta')|}. \quad (51)$$

Since $z_\zeta(\zeta)$ has a second-order pole at $\zeta = -i$, it is necessary that the quantity inside the brackets in expression (50), and its derivative, vanish at $\zeta = -i$ so that near $\zeta = -i$

$$I(\zeta, \operatorname{Ca}) + \frac{D}{\zeta^2} + \frac{C}{\zeta} - \overline{D}\zeta^2 - \overline{C}\zeta + ib = A(\zeta + i)^2 + \dots \quad (52)$$

for some complex constant A which is related to f_∞ by

$$iaA = f_\infty. \quad (53)$$

This means that

$$I(-i, \operatorname{Ca}) - D + \overline{D} + iC + i\overline{C} + ib = 0, \quad (54)$$

and

$$I_\zeta(-i, \operatorname{Ca}) + 2iD + C + 2\overline{D}i - \overline{C} = 0, \quad (55)$$

while

$$A = \frac{1}{2} \left[I_{\zeta\zeta}(-i, \operatorname{Ca}) + 6D - 2Ci - 2\overline{D} \right]. \quad (56)$$

Since $I(-i, \operatorname{Ca})$ is purely imaginary, (54) is a single real condition, namely, an equation for the real parameter b in terms of C and D .

If the map $z(\zeta)$ and the constants b , C and D are known, (51) gives an explicit expression for $F(\zeta)$. Condition (31) then provides the following expression for $G(\zeta)$:

$$G(\zeta) = -\overline{z}(\zeta^{-1})F(\zeta). \quad (57)$$

This condition is very revealing: it shows that the singularities of $G(\zeta)$ dictate the singularities of the conformal mapping function $z(\zeta)$. In particular, it shows that if $G(\zeta)$ has a pole singularity at $\zeta = 0$ then the functional form of the mapping function is finite. To see this suppose, for example, that $z(\zeta)$ has the special truncated form

$$z(\zeta) = \frac{a}{\zeta + i} + a_0 + \sum_{k=1}^n a_k \zeta^k, \quad (58)$$

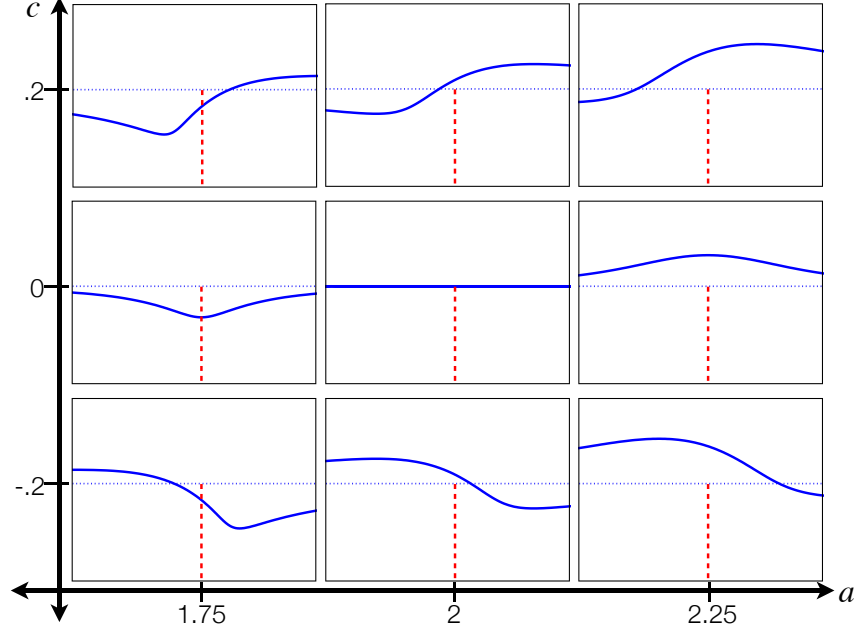


FIG. 4: The geometrical significance of parameters a and c . The flat interface corresponds to $a = 2, c = 0$. Increasing (decreasing) a above 2 with $c = 0$ (along the horizontal axis) moves the interface up (down) in a left-right symmetric fashion. Non-zero values of c (along the vertical axis) introduce left-right asymmetry.

where $n \geq 1$ is some positive integer. Then

$$\bar{z}(\zeta^{-1}) = \frac{\bar{a}\zeta}{1 - i\zeta} + \bar{a}_0 + \sum_{k=1}^n \frac{\bar{a}_k}{\zeta^k}. \quad (59)$$

Since $F(\zeta) = \mathcal{O}(\zeta^{-1})$ as $\zeta \rightarrow 0$, it follows from equation (57) and (59) that, near $\zeta = 0$, $G(\zeta)$ has the form

$$G(\zeta) = \frac{G_{-(n+1)}}{\zeta^{n+1}} + \frac{G_{-n}}{\zeta^n} + \dots + \frac{G_{-1}}{\zeta} + G_0 + G_1\zeta + \dots \quad (60)$$

implying that, near z_d ,

$$g(z) = \frac{g_{-(n+1)}}{(z - z_d)^{n+1}} + \text{higher order terms}. \quad (61)$$

Since our swimmer model means that $g(z)$ must have the form given in (14) it is clear that we must pick $n = 1$. The conformal map then has the form

$$z(\zeta) = \frac{a}{\zeta + i} + a_0 + a_1\zeta, \quad (62)$$

where a, a_0 and a_1 are complex numbers.

In addition, there are geometrical constraints on the conformal mapping parameters. Suppose that the singularity is at $z_d = -i$. This implies that $z(0) = -i$ and therefore that

$$a_0 = (a - 1)i. \quad (63)$$

Furthermore, the condition that the interface tends to $y = 0$ implies

$$\text{Re}[a_1] = \frac{a}{2} - 1. \quad (64)$$

Hence, the mapping function can be expressed as

$$z(\zeta) = \frac{a}{\zeta + i} + i(a - 1) + \left(\frac{a}{2} - 1 + ic\right) \zeta, \quad (65)$$

where a and c are two real parameters. These two parameters have the following geometrical interpretations. When $a = 2$ with $c = 0$ the interface is flat; increasing a above 2 corresponds to a symmetric *upward* deformation of the interface; decreasing a below 2 leads to a symmetric *downward* deformation. Changing the value of c away from zero introduces left-right *asymmetry* of the free surface deformation about a vertical axis through the swimmer, as illustrated in Figure 4.

The velocity of the swimmer in the co-moving frame is given by the finite part of the expression $u + iv$ at $z = -i$ and, for a steady solution, this must vanish. If

$$f(z) = \frac{s^*}{z + i} + f_0 + f_1(z + i) + \dots, \quad g(z) = \frac{q^*}{(z + i)^2} + \frac{(-is^* + d^*)}{(z + i)} + g_0 + g_1(z + i) + \dots \quad (66)$$

the finite part of $u + iv$ at $z = -i$ is given by

$$-f_0 - if_1 + \overline{g_1} = 0. \quad (67)$$

The terms f_0 , f_1 and g_1 are given (using the residue theorem) as

$$\begin{aligned} f_0 &= \frac{1}{2\pi i} \oint_{\Gamma} \frac{F(\zeta)}{(z(\zeta) + i)} \frac{dz}{d\zeta} d\zeta, & f_1 &= \frac{1}{2\pi i} \oint_{\Gamma} \frac{F(\zeta)}{(z(\zeta) + i)^2} \frac{dz}{d\zeta} d\zeta, \\ g_1 &= -\frac{1}{2\pi i} \oint_{\Gamma} \frac{\overline{z}(1/\zeta)F(\zeta)}{(z(\zeta) + i)^2} \frac{dz}{d\zeta} d\zeta \end{aligned} \quad (68)$$

where Γ is any simple closed curve surrounding $\zeta = 0$. Note that with $F(\zeta)$ determined from equation (50), $G(\zeta)$ from (57) and f_0 , f_1 and g_1 from (68), condition (67) is a linear equation for constants C and D . It should also be pointed out that f_0 , f_1 and g_1 can, in principle, be found in analytical form but the algebra involved is lengthy and it is easier to make use of the integral expressions (68) to compute these quantities.

If the values of a , c and U are specified, C and D can be found by simultaneously solving

$$-f_0 - if_1 + \overline{g_1} = 0, \quad (69)$$

which is a complex equation, together with the real equation (55), i.e.,

$$I_{\zeta}(-i, Ca) + 2iD + C + 2\overline{D}i - \overline{C} = 0, \quad (70)$$

and the real equation

$$-\frac{1}{2} = \text{Re} \left[\frac{ia}{2} \left[I_{\zeta\zeta}(-i, Ca) + 6D - 2Ci - 2\overline{D} \right] \right]. \quad (71)$$

With constants C and D determined in this way, functions $F(\zeta)$ and $G(\zeta)$ (and hence the flow field) are fully determined in analytical form. The stresslet, dipole and quadrupole strengths can then be readily computed to be

$$\begin{aligned} s^* &= D \left(\frac{3a - 2}{2} + ic \right)^2, \\ q^* &= -D \left(\frac{a - 2}{2} - ic \right) \left(\frac{3a - 2}{2} + ic \right)^2, \\ d^* &= \left(\frac{3a - 2}{2} + ic \right) \left[iDa \left(-\frac{a}{2} + 3 + 5ic \right) - C \left(\frac{a - 2}{2} - ic \right) \left(\frac{3a - 2}{2} + ic \right) \right]. \end{aligned} \quad (72)$$

As a check on the solution scheme, it was verified that when $a = 2$, $c = 0$ (so that the interface is flat) we retrieved the values

$$s^* = 2i, \quad q^* = 0, \quad d^* = -4, \quad (73)$$

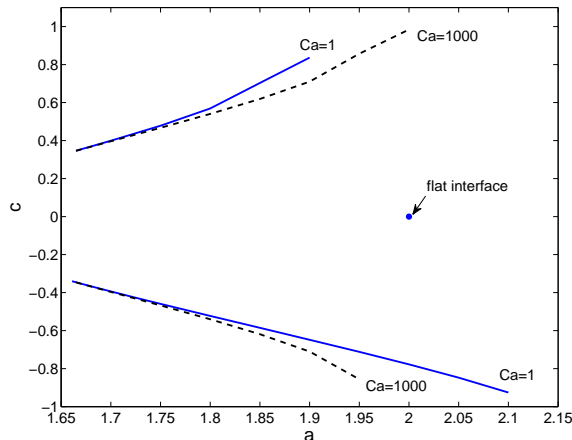


FIG. 5: The two solution branches: the values of c against a are plotted for $Ca = 1$ and 1000 . The upper branches have positive values of c , the lower branches have negative values of c . The flat interface parameters are also indicated to show that the actual solution branches are disconnected from it.

which are the values obtained in §IV using the method of images.

We have thus found that there is a two-parameter family of solutions, parametrized by a and c , for a force-free (but not necessarily non-rotating) point swimmer – characterized by a singularity description of the form (14) – steadily translating beneath a deformed free surface with speed $U = -1$.

It remains, however, to enforce the condition $\text{Im}[f_1] = 0$. In contrast to the case when the interface is assumed to be flat, we now have additional freedoms (in the choice of a and c) to enforce this condition. Physically, this means that possible equilibrium solutions exist within a two-parameter family of possible interface shapes. With a two-parameter family of possible solutions, and only a single additional requirement, we choose to specify a and see if there are any corresponding values of c such that $\text{Im}[f_1] = 0$. It must also then be checked *a posteriori* that the map (65) with these values of a and c are one-to-one (univalent) mappings to the fluid region. It has been found that such solutions do indeed exist. They are described in the next section.

VI. CHARACTERIZATION OF THE STEADY SOLUTIONS

For a given value of a , admissible values of c are found by insisting that

$$\text{Im}[f_1] = 0. \quad (74)$$

The nature of our formulation is such that the only stage in which we are required to solve a nonlinear equation is in satisfying (74). Newton’s method is used to satisfy this condition by fixing a value of a , taking a guess for c and then computing the associated functions $F(\zeta)$ and $G(\zeta)$ together with the values of f_0, f_1 and g_1 . The value of c is then updated iteratively until condition (74) is satisfied. It is then checked *a posteriori* that the resulting conformal mapping is a one-to-one mapping from the interior of the unit ζ -disc to the fluid domain.

Figure 5 shows a graph of c against a when $Ca = 1$ and $Ca = 1000$. Focussing on the case $Ca = 1$ first it is clear that there are two solution branches: for certain values of a (but not all) two possible values of c giving physical admissible solutions are found. This is not surprising given that a and c are simply mathematically convenient parameters that are related to physically meaningful parameters (e.g. the multipole strengths) via highly nonlinear relations.

The lower solution branch corresponds to $c < 0$: Figure 6 shows typical profiles throughout the range of existence of this branch and reveals that the point of highest curvature is to the right of the swimmer.

Figure 7 shows the magnitudes of the multipole strengths as a function of a for this branch of solutions. Interestingly, as $a \rightarrow 1.66$ which is the lowest a -value for which solutions are found to exist on this branch the free surface profile

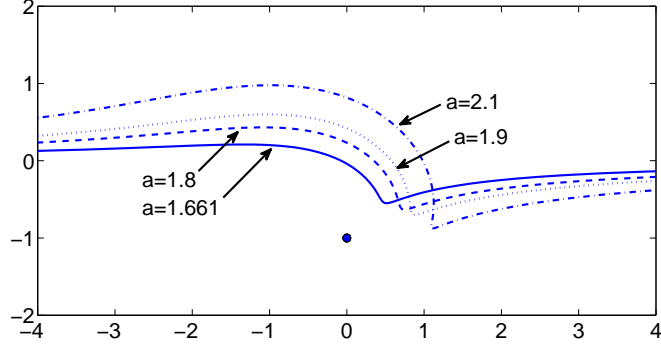


FIG. 6: Free surface profiles (with $Ca = 1$) for four different a in the range of existence of solutions for the lower solution branch in Figure 5 corresponding to c negative.

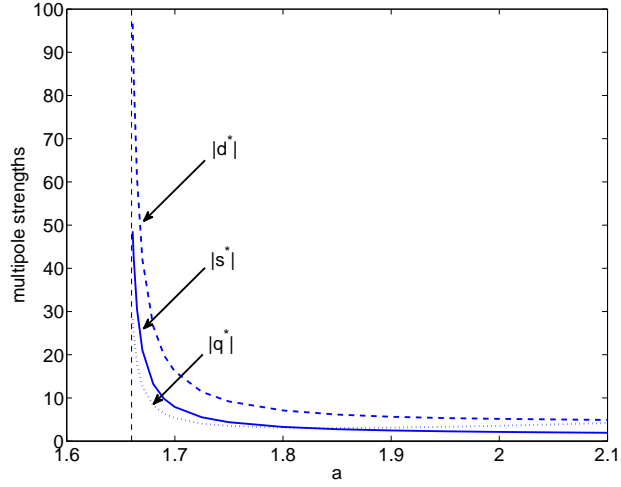


FIG. 7: Multipole strengths for $Ca = 1$ in the range of existence of solutions for the lower solution branch with c negative.

tends to a configuration in which the point of highest curvature tends to a finite value but the multipole strengths appear to grow without bound (hence the vertical asymptote shown in Figure 7). On the other hand, as a tends to the upper value for which solutions exist the value of the maximum curvature of the interface appears to grow without bound while the values of the multipole strengths appear to asymptote to finite values.

Figures 8 and 9 show similar graphs for the upper branch for which c is positive. Now the point of highest curvature on the interface is to the left of the swimmer position. The qualitative behaviour of the solution branch is very similar, however, to the lower branch just investigated. At one end of the range of existence of solutions the maximum curvature of the interface tends to a finite value with the multipole strengths growing without bound; at the other end of the range, the maximum curvature of the interface grows without bound with the multipole strengths levelling off to well-defined values.

The above results appear to be only weakly dependent on the capillary number Ca . Figure 5 also shows c against a in the case $Ca = 1000$ and once again two distinct solutions branches are found (disconnected from the flat state solution). One solution branch has $c < 0$, a second has $c > 0$. The free surface profiles for the two solution branches are depicted in Figure 10 and are qualitatively similar to the $Ca = 1$ case.

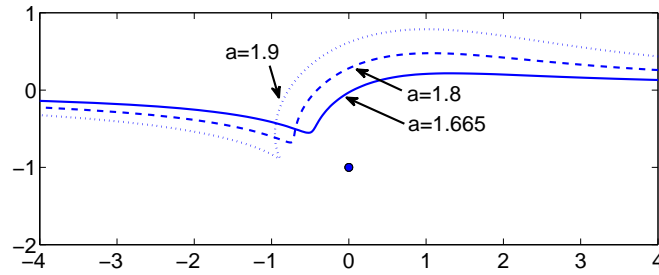


FIG. 8: Free surface profiles (with $Ca = 1$) for three different a in the range of existence of solutions for the upper solution branch in Figure 5 corresponding to c positive.

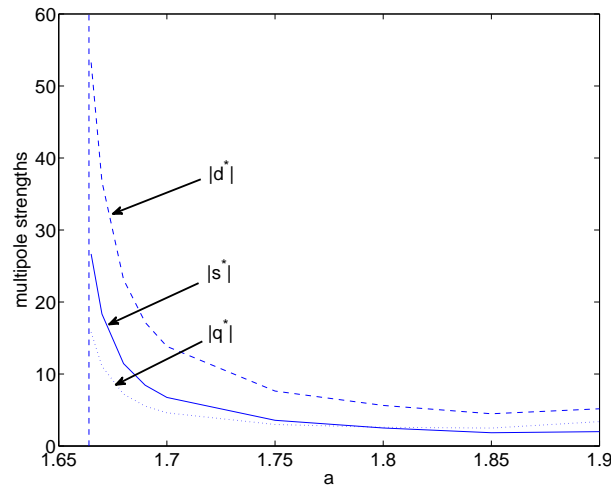


FIG. 9: Multipole strengths for $Ca = 1$ in the range of existence of solutions for the upper solution branch with c positive.

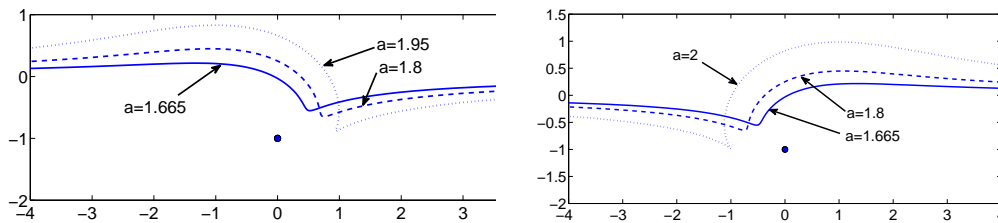


FIG. 10: Free surface profiles for the two solution branches with $Ca = 1000$ (left: lower branch; right: upper branch). Shapes are qualitatively similar to the $Ca = 1$ case (Figs. 6 and 8).

It appears therefore that modes of steady translation are possible and that they are associated with a range of free surface profiles. What is clear from the solutions is that the steady motion requires significant deformations of the surface. In other words, the nonlinear interaction between the swimmer and the deformability of the interface is crucial for steady swimming.

It is natural to ask which of the family of steady solutions might be realized in practice or be energetically preferable. Usually such matters are decided based on some definition of swimmer efficiency. An example is to minimize the energy dissipation associated with a displacement of the swimmer by unit distance. Unfortunately, owing to the fact that the model used here involves introducing singularities in the flow then the associated dissipation rates are unbounded (however, some progress in this direction has recently been made by [37] where use is made of the exact solution class found here). Nevertheless, it is intuitively sensible that the particular biological characteristics of any given swimmer will mean that there is an upper bound on the strength of the far-field multipoles in any effective singularity description of the swimmer. Moreover, it is also sensible to suppose that the rate of energy dissipation will be smaller when the multipole strengths are smaller. Figures 7 and 9 show that the multipole strengths are least when the values of a are greatest. As shown in Figures 6 and 8 it is for these higher values of a that the free surface tends towards a near-cusped interfacial shape (either in front of, or behind, the swimmer). These considerations suggest that efficient swimmers in steady motion will be inclined to produce free surface deformations exhibiting a region of high curvature.

VII. CONCLUSION

In this paper we have used complex analysis to identify a new mode of low-Reynolds swimming, namely organisms or devices that generate flow disturbances which exploit the deformation of a nearby free surface to swim steadily parallel to the interface. The resulting surface shapes are illustrated in Figures 6, 8 and 10. The two solution branches we obtain, displayed in Figure 5 are seen to be disconnected from the flat state solution. The interaction between the swimmer's disturbance to the flow, the free surface, and the subsequent swimmer's dynamics is highly nonlinear, and it is likely to be difficult to derive the solutions presented here by a weakly nonlinear perturbation analysis about the flat state. It is therefore of mathematical interest that by employing complex variable methods and a singularity model we have found these nonlinear interactions to be mathematically tractable.

The swimmer model we have used is motivated by a simple treadmilling circular motion of the kind first considered by [31]. In principle the mathematical techniques used here are extendible to more detailed and realistic singularity representations. Furthermore it should be possible to extend this study by using the method of matched asymptotic expansions to match an "inner" flow generated by a small finite-area swimmer with an "outer" solution in which the flow generated by that swimmer interacts with the free surface. The assumptions of such an analysis would be that the swimmer size is small compared to its distance from the interface so that, at leading order in an expansion based on a parameter expressing this ratio of scales, the swimmer would look like a point singularity. The solutions found here would then serve as the outer solutions in such a scheme. [38] has used precisely such a strategy of matched asymptotics in his two-dimensional complex variable model of a deformable bubble in the flow field generated by Taylor's four-roller mill.

The bearing of our two-dimensional analysis on the physics of actual organisms employing a free surface for propulsion is not clear. Other models for free surface locomotion have been proposed [24] also involving free surface interaction, but they were restricted to small-amplitude motion. Here, using a fully nonlinear analysis, we have unveiled an essential mechanism for the steady locomotion of a swimmer near a free capillary surface. In particular, our analysis has demonstrated the essential role played by interface deformability, and hinted at the significance of regions with high surface curvature.

It is likely that, as in the case of swimming near a no-slip wall, the generic locomotion mechanism of an organism near a free surface will have a more complicated spatio-temporal structure. Indeed, free surface deflection associated with unsteady undulatory waves propagating along the foot of a water snail have been observed in practice. In future work it may be interesting to study the full unsteady dynamics of a point swimmer near a free capillary surface. The geometrical complexities even in that simplified case would no doubt require a fully numerical investigation. An

analysis of the stability of the steadily translating equilibria just identified is also of interest but is left for a future study.

This work was funded in part by the US National Science Foundation through grants CTS-0624830 (EL and AEH) and CBET-0746285 (EL). DC acknowledges the support of an EPSRC Advanced Research Fellowship as well as the hospitality of the Department of Mathematics at MIT where this work was initiated. OS also acknowledges support from an EPSRC studentship.

-
- [1] C. Brennen and H. Winet. Fluid mechanics of propulsion by cilia and flagella. *Annu. Rev. Fluid Mech.*, 9:339, 1977.
 - [2] E. Lauga and T. R. Powers. The hydrodynamics of swimming microorganisms. *Rep. Prog. Phys.*, 72:096601, 2009.
 - [3] K. Maeda, Y. Imae, J. I. Shioi, and F. Oosawa. Effect of temperature on motility and chemotaxis of *Escherichia coli*. *J. Bacteriol.*, 127, 1976.
 - [4] H. C. Berg and L. Turner. Chemotaxis of bacteria in glass capillary arrays - *Escherichia coli*, motility, microchannel plate, and light scattering. *Biophys. J.*, 58:919–930, 1990.
 - [5] P. D. Frymier and R. M. Ford. Analysis of bacterial swimming speed approaching a solid-liquid interface. *AIChE J.*, 43:1341–1347, 1997.
 - [6] E. Lauga, W. R. DiLuzio, G. M. Whitesides, and H. A. Stone. Swimming in circles: Motion of bacteria near solid boundaries. *Biophys. J.*, 90:400–412, 2006.
 - [7] J. W. Costerton, Z. Lewandowski, D. E. Caldwell, D. R. Korber, and H. M. Lappinscott. Microbial biofilms. *Ann. Rev. Microbiol.*, 49:711–745, 1995.
 - [8] S. S. Suarez and A. A. Pacey. Sperm transport in the female reproductive tract. *Human Reprod. Update*, 12:23, 2006.
 - [9] A. J. Reynolds. The swimming of minute organisms. *J. Fluid Mech.*, 23:241–260, 1965.
 - [10] D. F. Katz. Propulsion of microorganisms near solid boundaries. *J. Fluid Mech.*, 64:33–49, 1974.
 - [11] D. F. Katz, J. R. Blake, and S. L. Paverifontana. Movement of slender bodies near plane boundaries at low Reynolds number. *J. Fluid Mech.*, 72:529–540, 1975.
 - [12] D.F. Katz and J.R. Blake. Flagellar motions near walls. In T.Y. Wu, C.J. Brokaw, and C Brennen, editors, *Swimming and Flying in Nature*, volume 1, pages 173–184. Plenum, New-York, 1975.
 - [13] L. J. Fauci and A. Mcdonald. Sperm motility in the presence of boundaries. *Bull. Math. Biol.*, 57:679–699, 1995.
 - [14] L. Rothschild. Non-random distribution of bull spermatozoa in a drop of sperm suspension. *Nature*, 198:1221, 1963.
 - [15] H. Winet, G. S. Bernstein, and J. Head. Observations on the response of human spermatozoa to gravity, boundaries and fluid shear. *J. Reprod. Fert.*, 70:511–523, 1984.
 - [16] J. Cosson, P. Huitorel, and C. Gagnon. How spermatozoa come to be confined to surfaces. *Cell Motil. Cytoskel.*, 54:56–63, 2003.
 - [17] D. M. Woolley. Motility of spermatozoa at surfaces. *Reproduction*, 126:259–270, 2003.
 - [18] J. P. Hernandez-Ortiz, C. G. Stoltz, and M. D. Graham. Transport and collective dynamics in suspensions of confined swimming particles. *Phys. Rev. Lett.*, 95:204501, 2005.
 - [19] A.P Berke, L. Turner, H.C. Berg, and E. Lauga. Hydrodynamic attraction of swimming microorganisms by surfaces. *Phys. Rev. Lett.*, 101:038102, 2008.
 - [20] Y. Or and R. Murray. Dynamics and stability of a class of low Reynolds number swimmers near a wall. *Phys. Rev. E.*, 79:045302, 2009.
 - [21] S. Zhang, Y. Or, and R. Murray. Experimental demonstration of the dynamics and stability of a low Reynolds number swimmer near a plane wall. *Proc. Amer. Cont. Conf.*, page (to appear), 2010.
 - [22] D.G. Crowdy and Y. Or. Two-dimensional point singularity model of a low Reynolds number swimmer near a wall. *Phys. Rev. E*, 81:036313, 2010.
 - [23] R. Trouilloud, T. S. Yu, A. E. Hosoi, and E. Lauga. Soft swimming: Exploiting deformable interfaces for low Reynolds number locomotion. *Phys. Rev. Lett.*, 101:048102, 2008.
 - [24] S. Lee, J. W. M. Bush, A. E. Hosoi, and Lauga E. Crawling beneath the free surface: Water snail locomotion. *Phys. Fluids*, 20:082106, 2008.
 - [25] G. K. Batchelor. The stress system in a suspension of force-free particles. *J. Fluid Mech.*, 41:545–570, 1970.
 - [26] T. J. Pedley and J. O. Kessler. Hydrodynamic phenomena in suspensions of swimming microorganisms. *Annu. Rev. Fluid Mech.*, 24:313–358, 1992.
 - [27] Y. Hatwalne, S. Ramaswamy, M. Rao, and Simha R. A. Rheology of active-particle suspensions. *Phys. Rev. Lett.*, 92:118101, 2004.
 - [28] J. Jeong and H. K. Moffatt. Free-surface cusps associated with flow at low Reynolds number. *J. Fluid Mech.*, 241:1–22, 1992.
 - [29] W.E. Langlois. *Slow viscous flow*. Macmillan, 1964.
 - [30] C. Pozrikidis. *Boundary Integral and Singularity Methods for Linearized Viscous Flow*. Cambridge University Press, 1992.
 - [31] J. R. Blake. Self propulsion due to oscillations on the surface of a cylinder at low Reynolds number. *Bull. Austral. Math.*

- Soc.*, 5:255–264, 1971.
- [32] M. Copeland. Locomotion in two species of the gastropod genus *Alectrion* with observations on the behavior of pedal cilia. *Biol. Bull.*, 37:126–138, 1919.
- [33] M. Copeland. Ciliary and muscular locomotion in the gastropod genus *Polinices*. *Biol. Bull.*, 42:132–142, 1922.
- [34] J. R. Blake. A note on the image system for a Stokeslet in a no-slip boundary. *Proc. Camb. Phil. Soc.*, 70:303–310, 1971.
- [35] J. R. Blake and A. T. Chwang. Fundamental singularities of viscous-flow. Part 1. Image systems in vicinity of a stationary no-slip boundary. *J. Eng. Math.*, 8:23–29, 1974.
- [36] M. Ablowitz and A.S. Fokas. *Complex variables*. Cambridge University Press, 1997.
- [37] S. Lee. *Biocomotion near free surfaces in Stokes flows: mechanism of swimming and optimization*. PhD thesis, Massachusetts Institute of Technology, 2009.
- [38] L.I. Antanovskii. Formation of a pointed drop in Taylor’s four-roller mill. *J. Fluid Mech.*, 327:325, 1996.

